Instrument Science Report WFC3 2012-13

TinyTIM Modeling of WFC3/IR Images

J. Biretta
July 09, 2012

ABSTRACT

We test the accuracy of TinyTIM version 7.4 for performing PSF modeling and subtraction on WFC3/IR data. These models are based on pre-launch laboratory tests, and have a number of issues when applied to on-orbit data. There are large residuals along the OTA spider diffraction spikes, which appear to be caused by the cold mask spider widths being ~20% too small in the model. There are also weaker patterns of rings which may be related to errors in the cold mask secondary size or centration. Excess coma is present in the models, and appears as a dark feature 2 to 6 pixels to the left of the star images. Finally the residuals show "speckle patterns" of bright and dark pixels at the center of the star which reach a maximum of 2% - 10% error. We have estimated the 5-sigma detection limit for identifying faint companions in TinyTIM subtractions, and it is about 6 magnitudes at 0.5 arcseconds from the star, and falls to about 9 magnitudes at 2 arcseconds, relative to the peak brightness of the star. These limits are several magnitudes poorer than obtained by other methods which subtract on-orbit observed PSFs from the target image. A future report will discuss improvements to the TinyTIM models.

Introduction

The TinyTIM package has been used for many years to simulate and model images produced by HST (Krist, Hook, and Stoerh 2011). It presents a potentially powerful tool for modeling and subtracting bright stars while searching for faint companions such as planets and disks -- since the models can be made to an arbitrarily small pixel scale, they are not subject to the usual undersampling problems which occur when subtracting observed stars from each other.

The WFC3/IR camera onboard HST covers a wavelength range from 0.98 to 1.66 microns, and has a 1024 x 1024 pixel detector array with ~0.13 arcsecond pixels. It has been incorporated into TinyTIM using laboratory measurements of the camera aberrations (Hook and Stoerh 2008), but the TinyTIM models have not been extensively tested using on-orbit data.

In response to observer questions, we investigate the accuracy of TinyTIM for modeling and subtracting stellar point spread functions (PSFs) from on-orbit WFC3/IR images. The next section discusses our procedure. The subsequent sections discuss the observations used for the tests, qualitative results, and finally quantitative results.

PSF Modeling and Subtraction Procedure

We use TinyTIM version 7.4 to generate a model PSF for each observed star image, and then use the procedure described below to align and scale it to the observed image. For reference, the aberration parameters for TinyTIM version 7.4 are listed in Appendix A. While a web interface for TinyTIM is available, it does not provide sufficient flexibility for our purposes. Instead we have downloaded and compiled the source code, and use that.

Since our goal is to ascertain the accuracy of TinyTIM, we must be careful to minimize errors from all other sources. Precise alignment of the TinyTIM model to the observed image is of critical importance for an accurate test; otherwise the subtraction may have large errors which are due to the test procedure itself, and not caused by TinyTIM. We have used a cross-correlation method (e.g. Biretta, Owen, and Cornwell 1989) which is highly sensitive to small position differences, to align the model PSFs with the observed star images. The technique used here, briefly summarized, is to shift a 10x over-sampled TinyTIM model PSF by 0.001 pixel (0.00013 arcsecond) increments, re-bin it to normal pixel size, and cross-correlate it against the observed star image until the shift is found which are maximizes the cross-correlation. In detail, the procedure is as follows:

1) Modeling of an observed star image begins with various parameters being extracted from the image header. These include the instrument, detector, aperture, filter, and the MJD of the exposure start and end.
2) The WFC3 focus is determined by computing the MJD at the middle of the exposure, and then interpolating in tables of the HST focus which were kindly provided by Colin Cox[1]. The tables give the HST focus averaged amongst the different instruments

[1] Tables of the HST focus for each calendar year have since been made available at http://www.stsci.edu/hst/observatory/focus/FocusModel under "Annual Summary." Typical uncertainties

sampled at 5 minute intervals throughout the lifetime of WFC3. A small correction (-0.24 microns) is made from the average HST focus to the WFC3/UVIS focus. We have not made any correction from the WFC3/UVIS to the WFC3/IR focus.

3) An automated search algorithm is run on the image to locate the brightest star, which is assumed to be the target. During this process hot pixels, some of which are extremely bright, are rejected. The accuracy of the star location at this stage is about 1 pixel.
4) We intentionally reject images where the star is less than about 30 pixels from the sub-array edge, as these would make later stages in the analyses difficult. Many of the 128 x 128 sub-array images from 2009 were rejected for this reason.
5) TinyTIM does not know about WFC3/IR sub-arrays, hence the position of the star in the full-frame 1014 x 1014 pixel image is needed for estimating the field-dependent aberrations. The position on the full detector array is computed from the rough position in step 3 and the aperture name in the image header.
6) TinyTIM program "tiny1" is run[2]. Inputs include the HST camera, the effective position of the star in the full frame image, the filter, the spectral class of the target star, and the HST focus. This program generates a parameter file which is used by subsequent steps in TinyTIM.
7) TinyTIM program "tiny2" is run. This calculates an undistorted PSF sampled with pixels 1.3 times finer than the Nyquist sampling rate at the shortest wavelength in the filter pass band.
8) TinyTIM program "tiny3" is run using the output of "tiny2." This generates a geometrically distorted PSF, which we have specified to be sampled with 0.013 arcsecond pixels (10x over-sampled). As with all TinyTIM models, the output PSF is centered in the PSF image, and is centered at a pixel center. This is true regardless of the position supplied in step 6, which is only used to estimate the position-dependent aberrations.
9) Accurate alignment between the observed star and model PSF on the pixel grid are critical to generating a good model, so the next several steps involve aligning the model PSF to the observed star. This process begins by generating a copy of the observed image with 0.013 arcsecond pixels (10x oversampled), and replacing the star image with the TinyTIM model PSF at approximately the correct location on the pixel grid.

---

in the focus values for WFC3 are about 1.3 microns in units of HST secondary mirror de-space (Cox and Niemi 2011).

[2] The user-compiled version of TinyTIM has three separate programs called tiny1, tiny2, and tiny3 which are typically run in that order. Tiny1 sets parameters which are used by tiny2 to generate the model PSF, and finally tiny3 resamples the PSF to the desired pixel size and applies the instrument's geometric distortions.

10) This 10x oversampled model of the star is shifted using IMLINTRAN in IRAF to adjust and correct its position on the detector pixel grid. Spline interpolation is used. Initially this correction is zero, but it is updated as alignment iterations progress.
11) If desired, intra-pixel QE variations of the detector can applied to the model at this point. As of this writing we have not incorporated intra-pixel response variations since the current consensus is that there are none in the WFC3 IR detector (McCullough and Bushouse 2008; Pavlovsky, McCullough, and Baggett 2011).
12) The model image is re-binned to normal detector pixels (0.13 arcseconds) using IRAF BLKAVG. This does not involve any interpolation, but only a simple summing of the pixels.
13) A 3x3 pixel convolving kernel is applied to the model image to simulate the effects of inter-pixel capacitance in the WFC3/IR detector. TinyTIM will normally perform this step internally, but since we are requesting an over-sampled PSF, this step is automatically disabled within TinyTIM and is left for the user to perform manually. We used IRAF task CONVOLVE and applied the kernel given by Hook and Stoehr (2008) [3]:

0.002	0.038	0.002
0.038	0.840	0.038
0.002	0.038	0.002

14) An iterative coarse position adjustment of the TinyTIM PSF on the pixel grid is then performed to better align it with the observed star image. The position of the star in both the observed and model images are measured using IRAF task IMCENTROID, a correction to the alignment is estimated, and steps 9 – 14 are iterated with the position correction in step 9 being updated and improved at each iteration. IMCENTROID is used merely to detect a "null" shift between the observed and model images; the shift values it produces need not be highly accurate in an absolute sense; we only rely on it giving the same answer for two similar images with the same shifts. IMCENTROID uses a one-dimensional centroiding algorithm on each axis. This step is intended only to provide a coarse alignment accurate to ~0.01 detector pixel. Iterations are halted when the centroids of the observed and model star agree to within 0.002 pixel.

[3]We used the Hook and Stoehr (2008) kernel as it gave the smallest PSF subtraction errors in our initial tests. Hilbert and McCullough (2011) give a much sharper kernel. A third kernel, with intermerdiate sharpness between the other two, appears internally in TinyTIM (c.f. the wfc3_ir.pup table quoted in Appendix A). We have not made an exhaustive study of this subject, and it might be possible to trade-off kernel sharpness with other sources of image blur, e.g., use a sharper kernel together with more de-focus or spherical aberration.

Typically about a dozen of these coarse alignment iterations are performed, though we allow up to 100 iterations before deciding the alignment failed.

15) Next a fine alignment is performed using a more-accurate but slower cross-correlation method with 0.001 pixel resolution. 5x5 pixel patches centered on the star from the observed and model images are cross-correlated. The normalized cross-correlation is computed for a shift of -0.001, 0, and +0.001 pixel applied to the model image in step 9 on both the X and Y axes. If the maximum correlation is not at zero shift, the shift correction in step 9 is updated by 0.001 pixel, and steps 9, 10, 11, 12, 13, and 15 are iterated until the maximum cross correlation occurs at zero shift. As with step 14 the cross-correlation method is used only to detect a null shift between the observed and model images. Typically 10 to 20 of these fine alignment iterations are used, though we allow up to 100 iterations before deciding the alignment failed. It is important to note that at no time are we interpolating the under-sampled image with 0.13 arcsecond pixels; all interpolation is done on the 10x over-sampled PSF image with 0.013 arcsecond pixels in step 10.
16) Once the observed and model images are aligned, the intensity scale of the model is adjusted to match that of observed image. Both the median background level throughout the image, and the total counts in the inner 5x5 pixels around the star are computed. This is done for both the observed and model images, and the background level and scale of the model are adjusted so as to bring them into agreement.
17) At this point the model of the observed image is complete, and we make various comparisons between it and the original observed image. For display purposes, a set of 51 x 51 pixel images are computed which are centered on the star. These displays include logarithmic scalings of both images, computed as $\log_{10}$(image), a difference between these log images, and a simple difference between the original linear images.
18) Finally various statistical parameters are computed for the simple linear difference between the observed and model images. The difference image is divided into five radial zones; these are $r \leq 3$, $3 < r \leq 5$, $6 < r \leq 9$, $9 < r \leq 12$, and $12 < r \leq 18$ pixels from the peak of the star image. These correspond roughly to radii of 0, 0.5, 1, 1.4, and 2 arcseconds. In each zone the maximum difference and RMS difference are computed with rejection of pixels flagged in the data quality file (i.e. extension [3] of the input image).

In the interest of efficiency, we have coded the above steps 1 – 18 into an IRAF "tiny.cl" package containing ~1700 lines of code. The user simply supplies the input image name and the star's spectral class, and the PSF modeling and subtraction are carried out in an automated fashion. Run times are typically 2 minutes per star on a four-processor 2.66 GHz Mac Pro 1.1.

Much effort went into testing the accuracy of our automated PSF modeling procedure. Perhaps the most critical property of the procedure is its ability to accurately derive the

position of the observed star and subtract it with very small residuals. This was tested as follows. Starting with an observed image, we replaced the extension [1] science data with a TinyTIM model where both the intensity and position of the star on the pixel grid were precisely known. The automated modeling procedure was then run on this test image, and the difference between the input and final model was examined. Twelve different models were run in this way with the star placed at different fractional pixel positions near the detector center. The largest error was 0.003 pixel in the position of the star, and 1.4% in intensity. The average errors were 0.002 pixel and 0.5% in intensity. This gives us some estimate of the accuracy of the test procedure itself, and some confidence that the larger errors found for modeling real star images are not due to inadequacies in the test procedure itself.

WFC3/IR Images Used for Tests

We used archival WFC3/IR images of bright stars for testing. The data sources are summarized in Table 1. These images are from either PSF or photometric calibration proposals. Both stars are white dwarfs. In most cases they were located near the detector center; however, proposals 11439, 11921, and 12701 use a 5-point grid with images near the detector center and towards each corner of the detector, as indicated in Table 1. The observations for proposal 11439 have been previously discussed in some detail by Hartig 2009, who used them to evaluate the on-orbit PSF quality. The data in 11451 have been previously used for photometric calibration (Kalirai, et al., 2009).

Only images in proposals 11439, 11921, and 12701 (25 images total) are deep enough to reveal details of the PSF structure beyond ~1 arcsecond from the star[4].The field center is probably the most interesting location in terms of studying the performance for GO observations, but between these proposals there are only three well exposed images at the field center in F098M, and two images in F160W. The other proposals provide large numbers of images taken at the field center, but are not very deep – one must either confine study to the inner ~1 arcsecond of the PSF, or average large numbers of images.

Images with the star very near the edge of the sub-array, within ~30 pixels of the edge, were rejected since they would make statistical analyses more complicated; this primarily affected the early data from 2009. Table 1 lists the numbers of images actually used for the analyses, not the total number available in the proposals.

[4]These deep images are made with SAMP-SEQ=STEPxxx to avoid saturating the PSF core.

Table 1. Star images used for PSF subtraction tests.

Star	Prop. ID #	Image Names	Filters	Approx. Observation Dates	Number of Images Modeled	Star Location on Detector	Notes
GD153	11439	IABL*	F098M, F160W	7/2009	10	5-pt grid	Long exposure, Hartig 2009
	11451	IAAC*	All	7-8/2009	48	Center	
	11921	IBBP*	F098M, F160W	6/2010	10	5-pt grid	Long exposure
	11926	IBCF*	All	12/2009 – 11/2010	191	Center	
	12334	IBNX*	F098M, F110W, F125W, F140W, F160W	3-7/2011	28	Center	
	12699	IBWI*	F098M, F110W, F125W, F140W, F160W	4/2012	10	Center	
	12701	IBTY*	F098M	11/2011	5	5-pt grid	Long exposure
GRW+70D5824	11557	IB5T*	F125W	2/2010	10	Center	
	12333	IBLL*	F098M, F105W, F110W, F125W, F140W, F160W	11/2010 – 10/2011	59	Center	
	12698	IBUC*	F098M, F105W, F110W, F125W, F139M, F140W, F160W	10/2011 – 3/2012	26	Center	

Qualitative Results of PSF Subtractions

We applied our modeling procedure to the ~400 images listed in Table 1. Here we briefly summarize some of the more interesting results. Figure 1 illustrates typical results for a well-exposed star image in the F098M filter. In general terms the model and observed star in panels (a) and (b) appear quite similar. However, subtracting the two images in panels c and d reveals a number of significant errors. Figure 2 shows similar results for an image in a long-wavelength filter, F160W. In both Figures 1 and 2 the (a) and (c) panels show single anomalous pixels which are detector artifacts. We begin by discussing the errors in qualitative terms, and later move to more quantitative discussions.

The difference images in panel (c) are the difference between the two logarithmic images in panels (a) and (b). Hence the brightest or darkest regions represent places where the error,

expressed as a fraction on the local value, is large. The displayed range of -1 to 1 encompasses values where the model is too bright or faint by a factor of 10. The most obvious errors in the log difference images (Figure 1c and 2c) are along the spider diffraction spikes, i.e. along 45 degree diagonals in the image. The spider diffraction spikes contain minima which are related to the thickness of the spider vanes, and these minima occur in different distances from the star center in the observed and model images. WFC3/IR instrument contains a cold mask which is used to block emission from the warm HST spider, and from the figures it is apparent that the cold mask spiders are too thin in the TinyTIM model. The distance from the star center to the first minimum in the spider diffraction pattern is about 20% larger in the TinyTIM model than in the observed image, which implies that the cold mask spider thicknesses are about 20% too small in the TinyTIM model[5].

For both filters the inner ~1.5 arcsecond radius shows evidence of bright and dark concentric features or rings, and these are on a scale comparable to that of the HST secondary mirror obscuration. Hence it seems likely that there is also some modest error in either the diameter or centration of the cold mask secondary mirror.

A more subtle error is also apparent in Figures 1c and 2c closer to the star center. In both filters the log difference images have a dark region from ~2 to ~6 pixels on the left side of the star center. Careful examination of Figure 1b shows the light distribution 2 – 3 pixels from the star center is asymmetric, with more light on the left side of the star than on the right. A similar situation was seen in virtually all ~400 images we processed. This type of error is a signature of coma aberration -- apparently there is more coma aberration in the TinyTIM models than in the observed images[6].

The difference images in Figure 1d and 2d are simple subtractions of (observed – TinyTIM) images, and are scaled so the range is from -10% to +10% of the peak brightness. The largest errors as a fraction of the peak brightness occur very near to the center of the star. In both Figures 1d and 2d the largest errors are about 5% of the peak intensity. This is much larger than the maximum 1% error we found while testing our procedures, hence it is certain these errors arise in the TinyTIM models and not the analysis procedure. Subtraction errors near the star center can arise from a wide range of sources. Errors in the low-order aberrations (i.e. focus, coma, astigmatism) are a potential contributor. Also, since brightness gradients are very large near the star, any errors while interpolating or binning the model PSF can have a large effect. HST pointing jitter is another potential contributor, though similar errors were seen even in very short exposures (1 – 2 seconds). Similar errors were seen in all of the ~400 images we tested, with the maximum error in each image ranging from ~2% to ~10% of the

[5] The relationship between spider thickness and diffraction minima distance is inverted since the obscurations and image are related through a Fourier transformation.

[6] Both the images at the detector center, and the ones near the detector corners, show excess coma.

peak brightness. These errors appeared to change randomly from one image to another, except that a string of repeated exposures in the same filter and pointing tended to all have similar errors with the same pattern of high and low pixels. It is almost as if there were an interpolation error somewhere in the modeling process whose error depends upon exactly where the star lands on the pixel grid. We will refer to these errors as a "speckle pattern" errors. Their exact cause is not yet known.

There are a total of three deep images available in the F098M filter near the detector center. We have averaged these and the result is shown in Figure 3. (This is a simple average of each display panel for the three input images.) This average image is probably the deepest un-saturated image that can be obtained with the archival data. Most of the features beyond the inner few pixels previously seen in Figure 1c persist in the average image and appear in Figure 3c. The apparently random errors at the inner few pixels, our so-called "speckle pattern" errors seen in Figure 1d, have averaged down and appear weaker in Figure 3c. The maximum error here is now ~2%.

It is interesting to examine the results when large numbers of images are averaged. This gives some indication of what features are persistent and which are somehow related to the circumstances of an individual observation. It also gives some idea of the results that might be obtained if a large number of position dithers could be obtained. Figure 4 shows such results for star GD153. Each of the 302 GD153 images listed in Table 1 was modeled. The observed images were then averaged, and the logarithm of the result is shown in Figure 4a. Pixels flagged in the data quality file (DQF, extension [3]) were omitted during this averaging. Similarly all the TinyTIM models were averaged, and the logarithm of the result is show in Figure 4b. The difference between these logarithms is shown in Figure 4c and the simple linear difference between the averages is shown in Figure 4d. Wavelength-dependent effects, such as the minima in the spider diffraction patterns, tend to smear-out and be reduced in these images, since data from a wide range in wavelength are averaged together. All images received the same weighting in the average, hence the noise is rather high in the outlying regions, which reflects the relatively low signal-to-noise of typical images. Nonetheless, the region within ~1 arcsecond of the star has a reasonable signal-to-noise ratio, and shows some interesting features. The coma feature mentioned before persists in the average images – a dark feature is seen on the left side of the star , roughly 2 – 6 pixels from the star, in Figures 4c and 4d. A similar bright feature is also seen on the right side of the star. The brightest features in Figure 4d are about 1% and significantly weaker than the 2% - 10% "speckle pattern" errors seen in individual PSF subtractions. Apparently averaging large number of images has greatly reduced some errors, such as those possibly related to interpolation on the pixel grid, while leaving errors related to model aberrations relatively unchanged.

Figure 5 shows the results for averaging all 95 images of GRW+70. The results are nearly identical to those for GD153 in Figure 4. The detailed pattern of bright and dark pixels near

the star center are nearly identical in Figures 4 and 5. This indicates the position-variable component of the "speckle pattern" error has mostly averaged away, leaving these patterns which are due to persistent errors in the model aberrations.

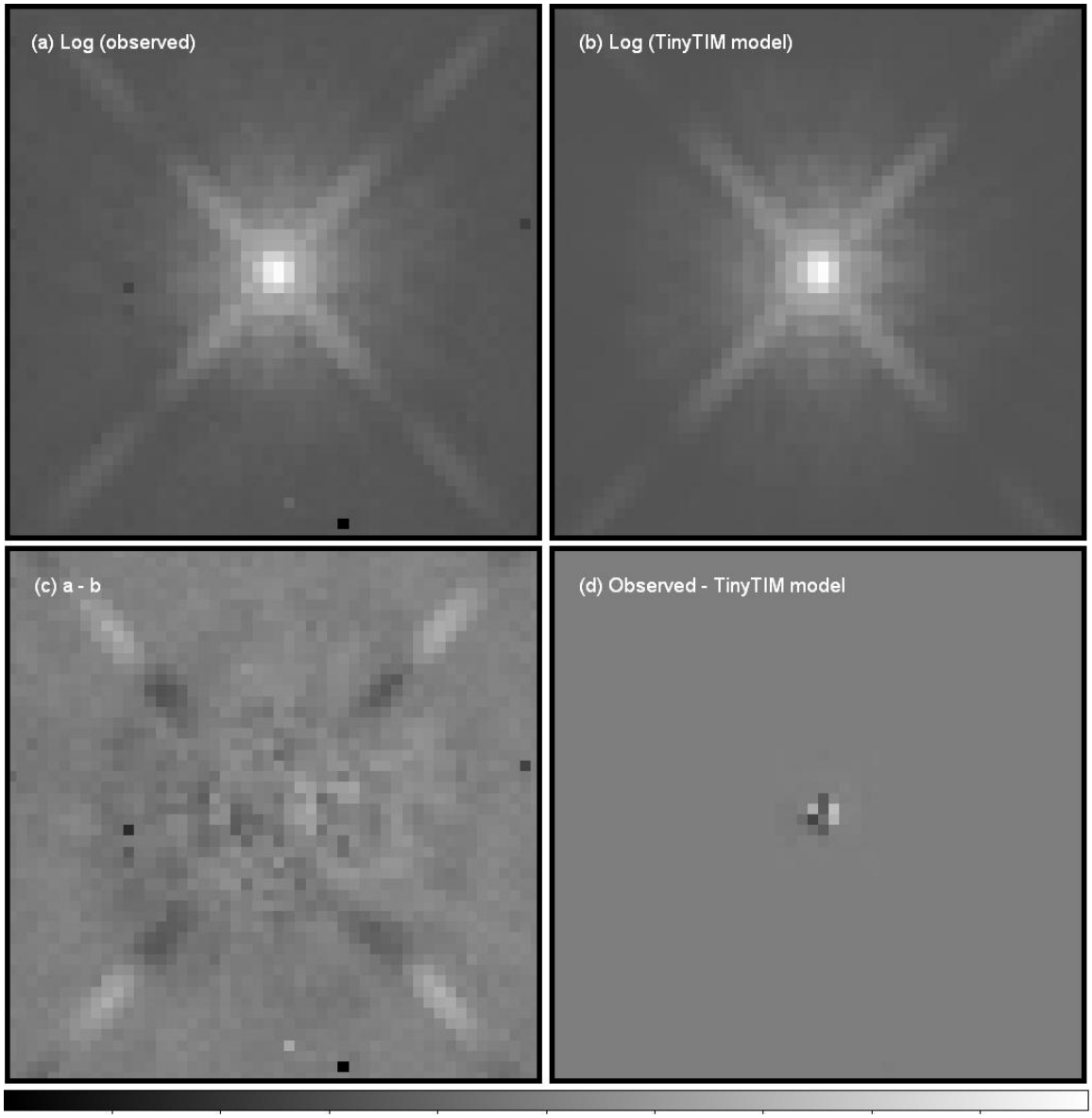

Figure 1. Results for the F098M filter with star GD153 placed near the detector center (archive image iabl01d7q). Displays and brightness ranges are as follows: (a) $\log_{10}$ display of the observed image with the peak pixel scaled to unity and display range -6 to 0; (b) same as panel (a) but for the TinyTIM model, (c) difference of panels (a) and (b) with display range -1 to +1, (d) simple ratio of the observed image divided by the TinyTIM model with display range -10% to +10%. Each image is 51 x 51 pixels in size, or ~7 arcseconds wide by ~6 arcseconds high; the different horizontal and vertical scales are due to geometric distortion.

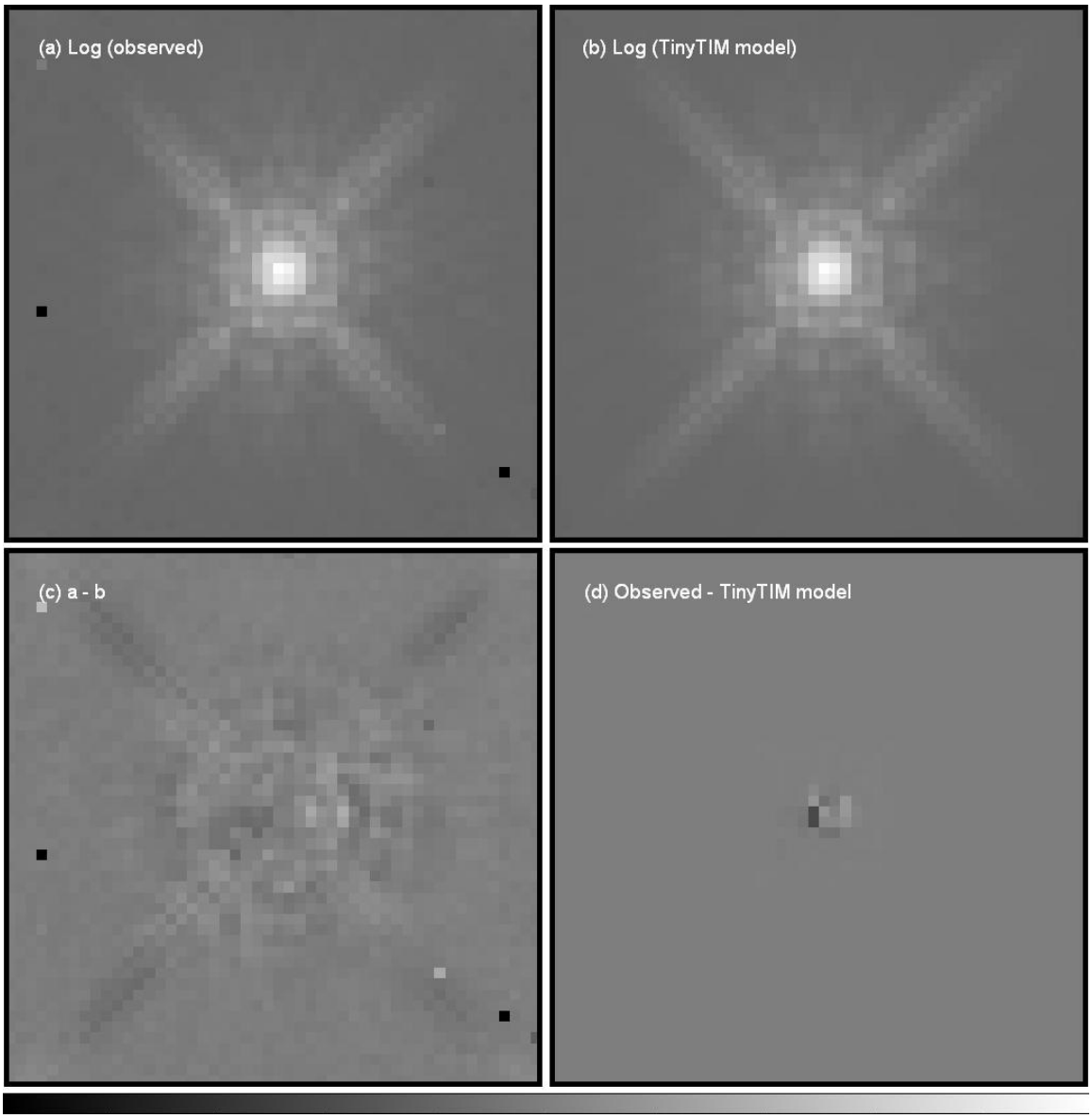

Figure 2. Results for the F160W filter with star GD153 placed near the detector center (iabl01d8q). Display brightness ranges and image sizes are the same as Figure 1.

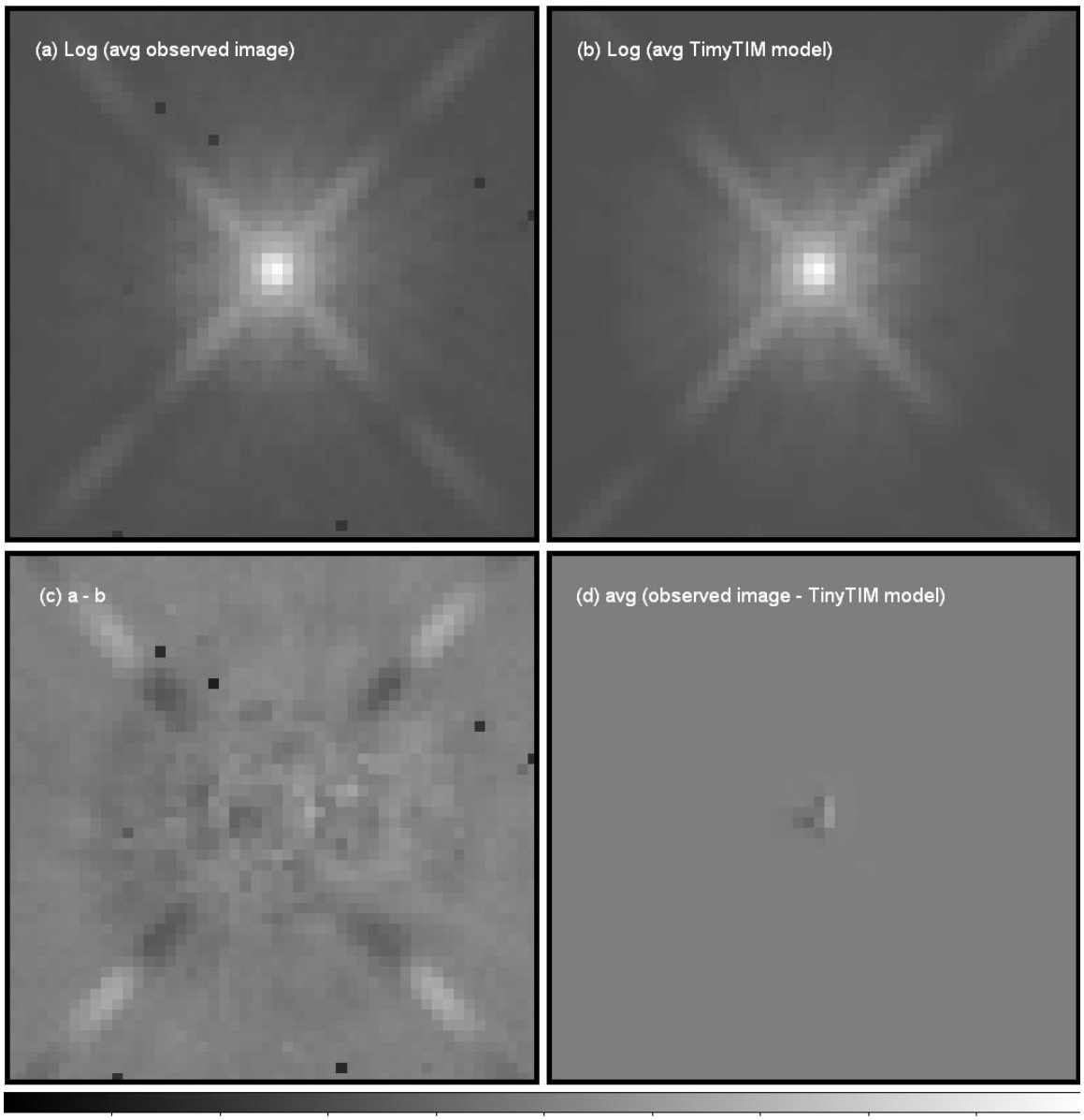

Figure 3. Similar to Fig. 1, but for an average of three deep F098M images of GD153 at the detector center (iabl01d7q, ibty03bdq, ibbp01iyq). Display brightness ranges and image size same as Figs. 1 and 2.

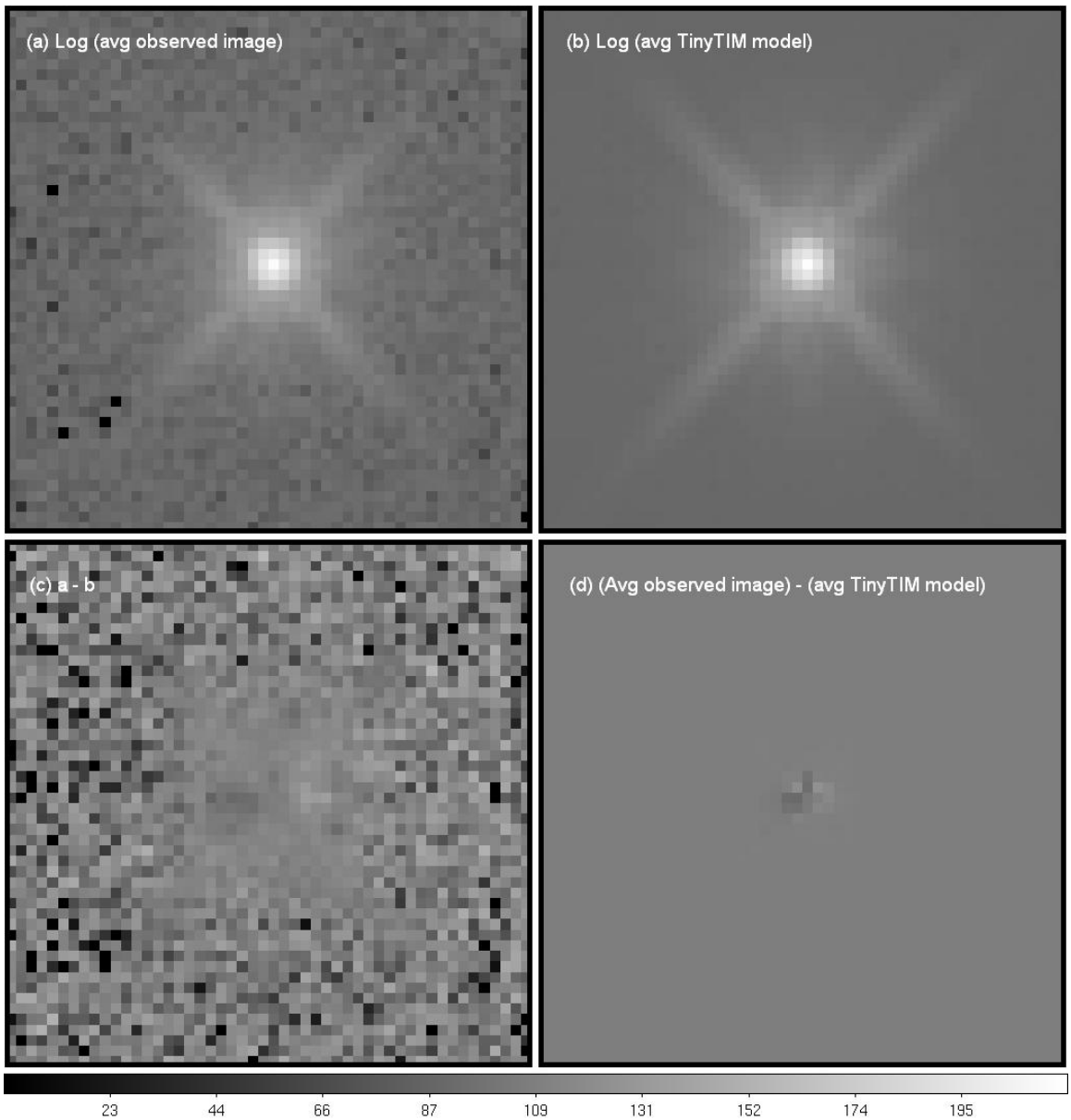

Figure 4. Similar to Fig. 3, but for an equally weighted average of all 302 GD153 images listed in Table 1. Display brightness ranges and image size same as Figs. 1 - 3.

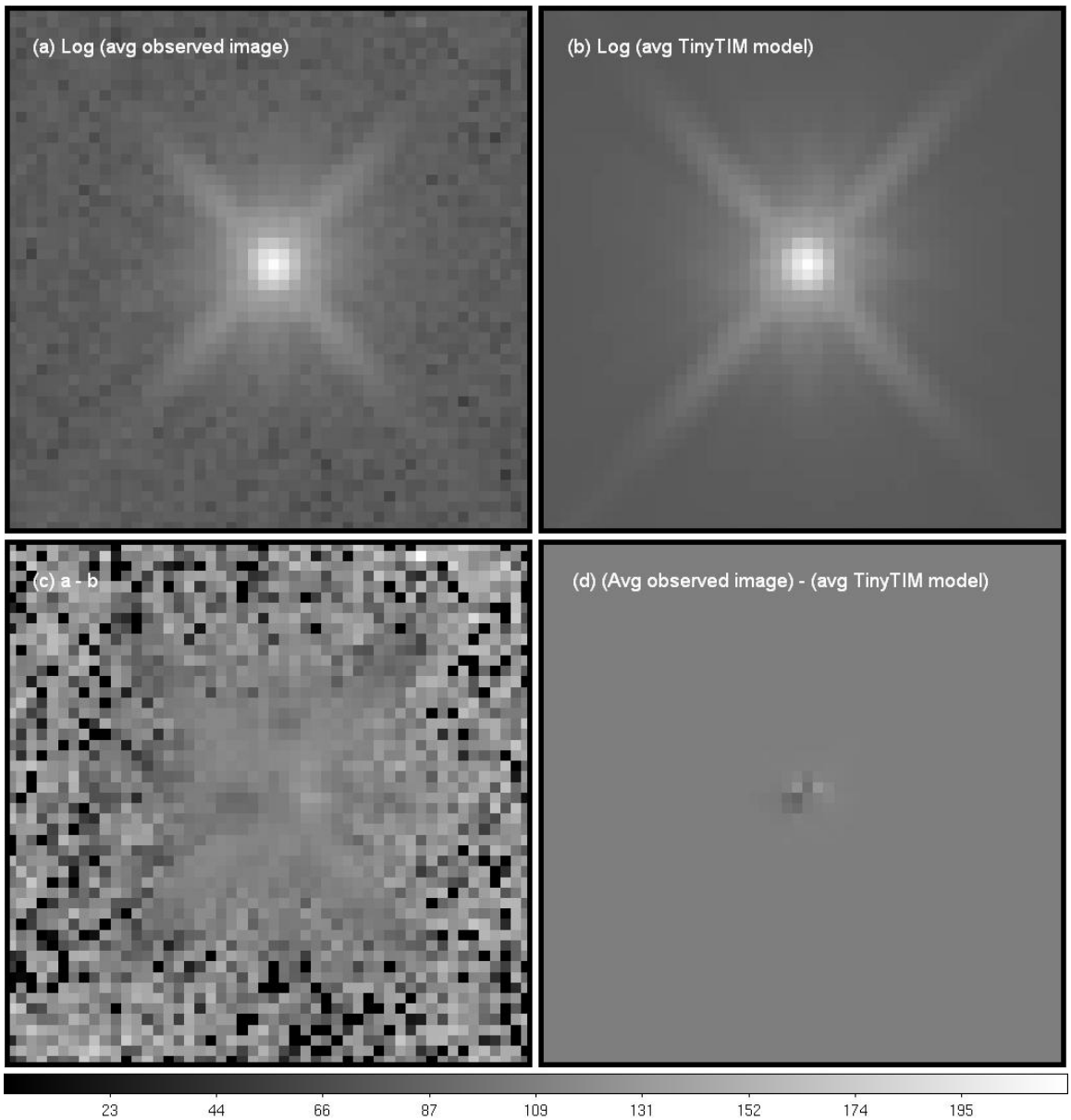

Figure 5. Same as Fig. 4, but for an equally weighted average of all 95 GRW+70 images listed in Table 1. Display brightness ranges and image size same as Figs. 1 - 4 .

Quantitative Results of PSF Subtractions

We have estimated quantitative PSF subtraction errors by computing the RMS and maximum error in the simple linear difference images, i.e. (Observed image) – (TinyTIM model image) images, comparable to those shown in Figures 1d and 2d. These are computed for five radial zones as described in step 18 of the procedure. Figures 6 and 7 show the results for deep

F098M and F160W images, respectively, from proposal 11439. Near the PSF center the RMS errors are 4 to 5 magnitudes below the peak brightness of the star, which reflects RMS errors of 1% to 3% of the peak brightness. At radii of 2 arcseconds the RMS error has fallen below 10 magnitudes. The results for the two filters are quite similar, with F160W having slightly larger errors between 1 and 2 arcseconds.

If an observer were attempting to detect a faint stellar companion to a much brighter star, they might be more interested to know the maximum PSF subtraction error at a given radius. We have plotted these in Figures 8 and 9. These are computed simply as the absolute value of the largest single-pixel deviation between observed star and model, and then converted to magnitudes relative to the peak brightness of the star. Near the star, the errors are dominated by the "speckle pattern" errors and coma error mentioned before. At larger radii the cold mask spider errors dominate. Results are similar for the two filters[7].

Rajan, et al., 2011 have given quantitative estimates of PSF subtraction performance using the so-called "LOCI" technique for WFC3/IR images. This method uses a library of observed PSFs for subtraction, and selects among them so as to minimize the local residuals. It is of interest to compare their results against the TinyTIM subtractions herein. Figure 10 shows our RMS error results for F098M (Figure 6) scaled up by a factor of five to illustrate approximate 5-sigma error or detection limits. On the same plot we also show the 5-sigma detection limits for a 2-orient LOCI subtraction from Figure 2 of Rajan, et al., 2011 (shown here as the dashed line). The LOCI technique reaches 1 – 3 magnitudes fainter than our TinyTIM subtractions. However it is conceivable that with some modification and improvement, as well as the use of dithered images and multiple orients, TinyTIM might approach the performance to the LOCI method. This work, however, beyond the scope of this report.

[7] Of course, an observer could reduce the error from the spider by obtaining images at several roll angles, and discarding the spider regions when averaging the images.

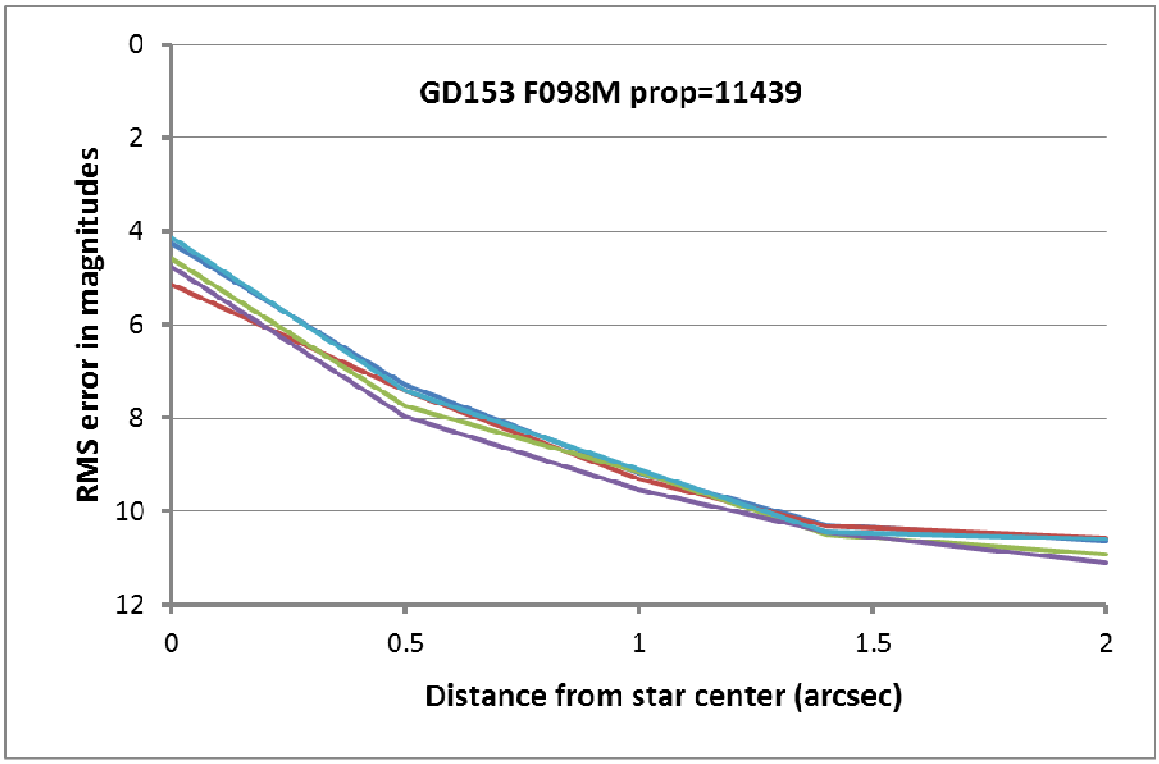

Figure 6. RMS PSF subtraction error vs. distance from star center. Each line represents one of five F098M images from proposal 11439 which are located near the detector center and near each corner. The errors are relative to the brightest pixel of the star image.

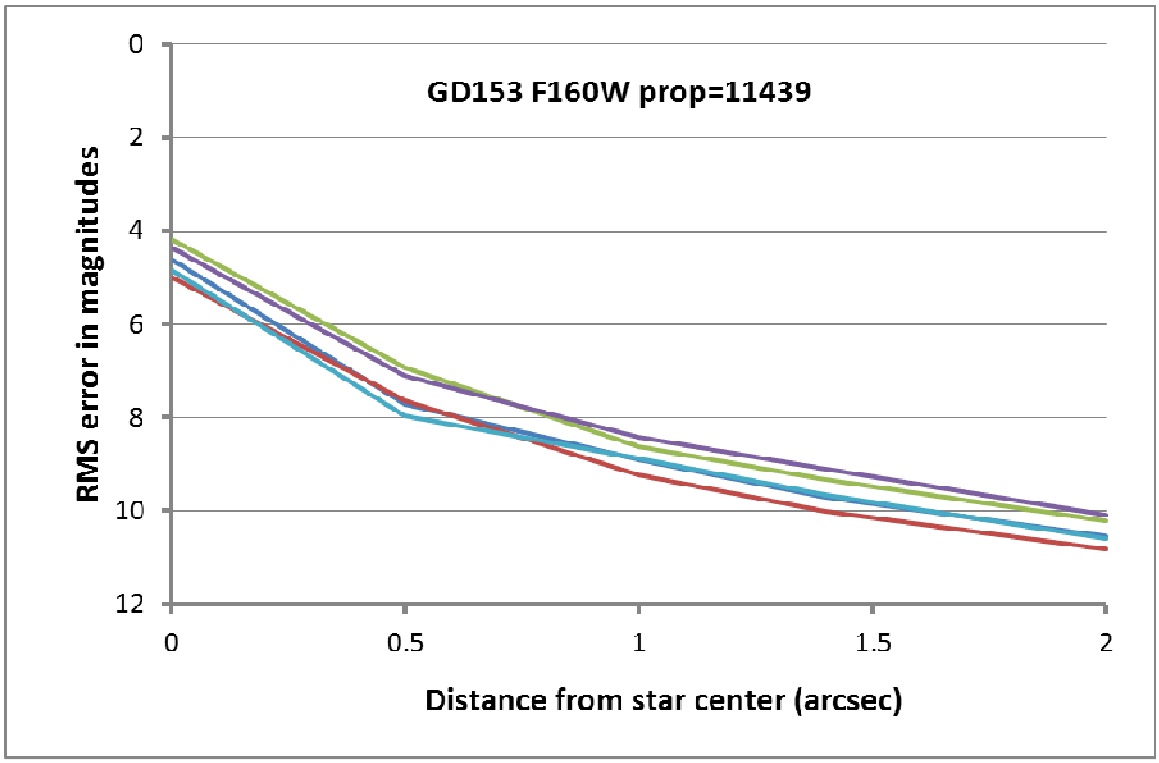

Figure 7. Same as Figure 4, but for five F160W images.

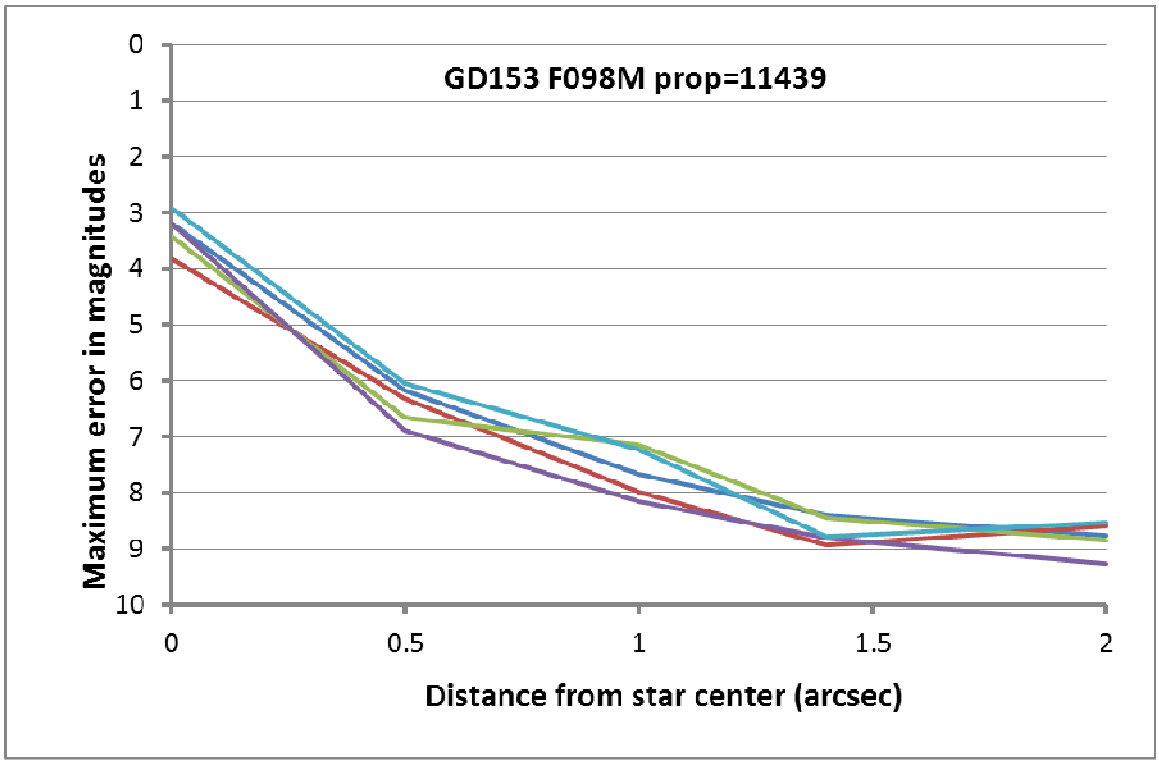

Figure 8. Maximum PSF subtraction error vs. distance from star center. Each line represents one of five F098M images from proposal 11439, which are located near the detector center and near each corner. The errors are relative to the brightest pixel of the star image.

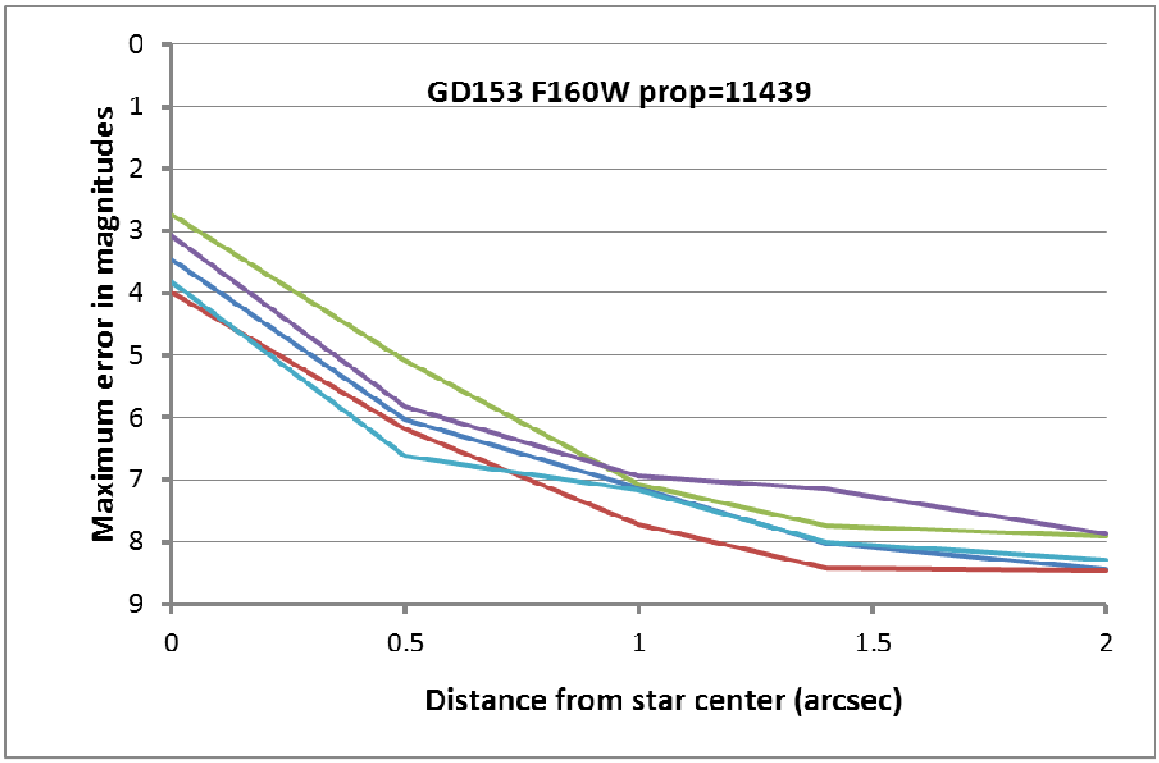

Figure 9. Same as Figure 4, but for five F160W images.

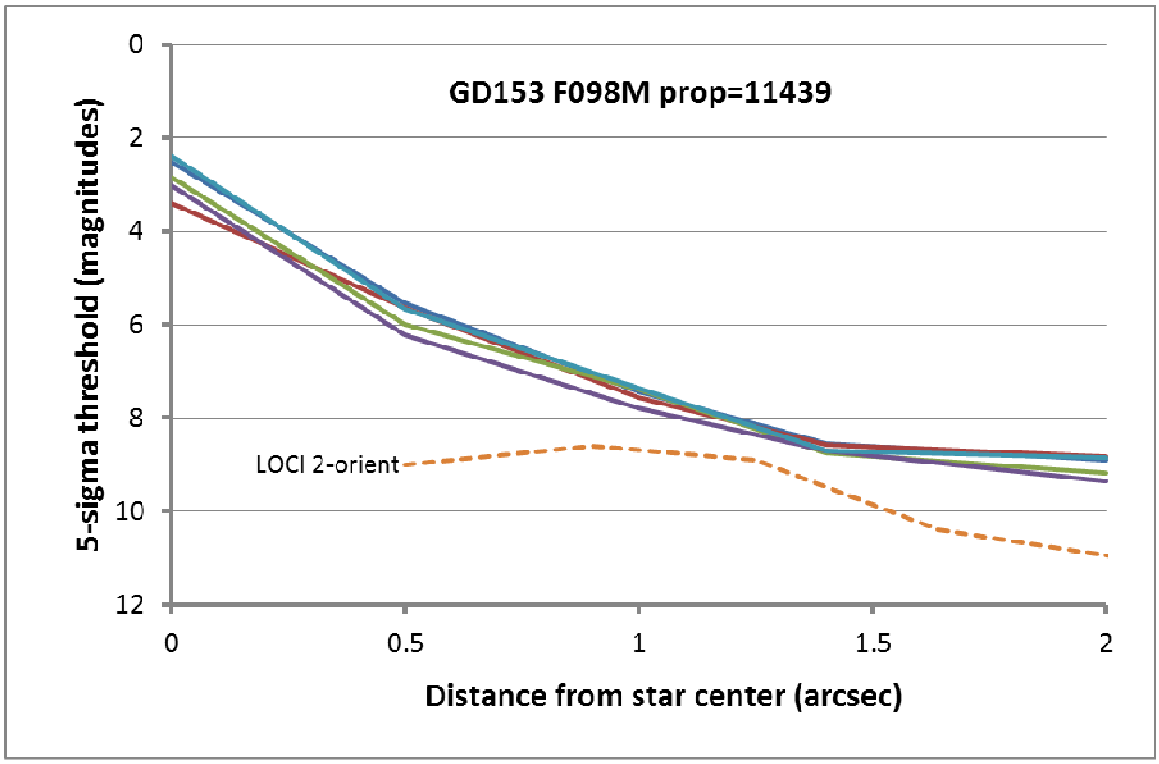

Figure 10. 5-sigma PSF subtraction limit vs. distance from star center. Details same as Figure 4. The dashed line illustrates the performance of LOCI 2-orient PSF subtraction from Rajan, et al., 2011.

Conclusions

We have tested the accuracy of TinyTIM version 7.4 for performing PSF modeling and subtractions on WFC3/IR data. The TinyTIM models are based on pre-launch laboratory tests, and have a number of issues when applied to on-orbit data. There are large residuals along the OTA spider diffraction spikes, which appear to be caused by the cold mask spider widths being ~20% too small in the TinyTIM model. There are also weaker patterns of rings in the residuals which may be related to errors in the cold mask secondary size or centration. The models also show excess coma, which appears as a dark feature 2 to 6 pixels to the left of the star images, with a similar bright feature on the right side of the star. Finally there are "speckle pattern" errors or bright and dark pixels in the subtractions at the center of the center of the star which reach 2% - 10% error relative to the brightest pixel of the star. These "speckle pattern" errors appear related to placement of the star on the pixel grid, and are greatly reduced when large numbers of images are averaged. These "speckle pattern" errors may be related to interpolation problems in the software.

An interesting use for TinyTIM is subtracting bright stellar objects and looking for faint

companions. We have estimated the 5-sigma detection limit for faint companions in TinyTIM subtractions and it is about 6 magnitudes at 0.5 arcseconds, and falls to about 9 magnitudes at 2 arcseconds, relative to the peak brightness of the star. These limits are several magnitudes poorer than other methods which have been applied to WFC3/IR data (e.g. LOCI method discussed by Rajan, et al., 2011).

It is likely that the performance of TinyTIM can be significantly improved by using on-orbit data to derive improved model parameters, as well as perhaps improving some of the internal interpolation methods, but this work is left to a future report.

We thank Colin Cox for providing tables of the HST focus, and Linda Dressel, George Hartig, John Krist, and Remi Soummer for helpful discussions.

References

Biretta, J. A., Owen, F. N., and Cornwell, T. J. 1989, ApJ 342, 128

Cox, C., and Niemi, S.-M. 2011, "Evaluation of a Temperature-Based HST Focus Model," ISR TEL 2011-01.

Hartig, G. F. 2009, "WFC3 SMOV Programs 11437/9: IR On-orbit PSF Evaluation," ISR WFC3 2009-37.

Hilbert, B., and McCullough, P. 2011, "WFC3 Instrument Science Report 2011-10 Interpixel Capacitance in the IR Channel: Measurements Made On Orbit," ISR WFC3 2011-10.

Hook, R. and Stoehr, F. 2008, "WFC3 Support in TinyTIM," ISR WFC3 2008-14

Kalirai, J. S. 2009, "WFC3 SMOV Proposal 11451: The Photometric Performance and Calibration of WFC3/IR," ISR WFC3 2009-30.

Krist, J. E., Hook, R. and Stoehr, F. 2011, Proc. SPIE, vol. 8127

McCullough, P., and Bushouse, H. 2008,"WFC3 TV3 Testing: IR Intrapixel Sensitivity," ISR WFC3 2008-29.

Pavlovsky, C., McCullough, P., and Baggett, S. 2011,"IR Intra-pixel Sensitivity Variance," ISR WFC3 2011-19

Rajan, A., Soummer, R., Hagan, J.B., Gilliland, R.L., and Pueyo, L. 2011, "High Contrast Imaging using WFC3/IR," ISR WFC3 2011-07

Appendix A: TinyTIM v. 7.4 WFC3/IR Aberration Tables.

Below we list the "as tested" aberration tables for WFC3/IR in TinyTIM version 7.4. Note the values for Zernikes Z4 – Z8 are not used, but instead the values of 1e-12 instruct the software to use field-dependent Zernikes in the wfc3_ir.pup table.

wfc3_ir.tab

```
# Zernike file for WFC3 IR Channel
# March 2008  Initial implementation (no aberrations)
# March 2011  Set Z4-Z8 terms to non-zero to activate coeffs in .pup file
  547.     # Reference wavelength (nm)
  22       # Last Zernike in file
  0.       # Z1 = (Not used)
  0.       # Z2 = X (V2) tilt
  0.       # Z3 = Y (V3) tilt
  1e-12    # Z4 = Focus
  1e-12    # Z5 = 0 degree astigmatism
  1e-12    # Z6 = 45 degree astigmatism
  1e-12    # Z7 = X (V2) coma
  1e-12    # Z8 = Y (V3) coma
  0.       # Z9 = X (V2) clover
  0.       # Z10 = Y (V3) clover
  0.       # Z11 = 3rd order spherical
  0.       # Z12 = 0 degree Spherical astigmatism
  0.       # Z13 = 45 degree Spherical astigmatism
  0.       # Z14 = X (V2) Ashtray
  0.       # Z15 = Y (V3) Ashtray
  0.       # Z16
  0.       # Z17
  0.       # Z18
  0.       # Z19
  0.       # Z20
  0.       # Z21
  0.       # Z22 = 5th order spherical
```

wfc3_ir.pup

```
# Pupil Table :  wfc3_ir.pup
# Do not change the order of these entries!
# Date : April 2008
# Preliminary version of WFC3 IR channel pupil information for Tiny Tim 7.0.
#
# Added preliminary distortion coefficients, from Colin Cox, March 2008
# Added preliminary cold-mask information from George Hartig, March 2008
#
# Date : Feb 2011
#  Swapped X/Y coeffs for astig and coma
#  Using charge diffusion kernel from WFC3 ISR 2008-41
# Date : March 2011
#  Updated V2,V3 (pupil) coordinates for reference position and camera center
#    using uab1537ci_idc.fits
#-------------------------------------------------------------------------
#
# Optical Telescope Assembly pupil information
#
 0.330  = OTA Secondary Mirror Radius
 0.022  = OTA Spider Width
#
# Mirror pad positions and radii
```

```
#
  0.8921  0.0000 0.065 = OTA Pad 1 (V3, V2, Pad Radius)
 -0.4615  0.7555 0.065 = OTA Pad 2
 -0.4564 -0.7606 0.065 = OTA Pad 3
#
# WFC3 IR wavelength range
#
  900 1700  = min, max detector wavelength (nm)
#
# WFC3 IR cold mask obscuration parameters
# These are from George Hartig, they are close, but not the same as the old
NICMOS ones.
#
 0.354 = WFC3 IR Secondary radius
 0.061 = WFC3 IR Spider width
 0.9755 = WFC3 IR Outer radius of cold mask
#
# Mask position
#
 0.0 0.0 = Mask X,Y positions
#
# WFC3 IR camera rotation (relative to OTA)
#
  135.0  = WFC3 IR camera rotation
#
# Pixel size (arcsecs)
#
   0.13 = WFC3 IR pixel size
#
# Axial offset of WFC3 IR camera
#
  0.0 0.0 = WFC3 IR Camera 2 V2,V3 axial offset
#
#  WFC3 IR field dependent aberration coefficients (in microns)
#
# Focus
#
-1.20318149e-02 -1.01187543e-04 7.07476814e-07 0.0e+00 0.0e+00 0.0e+00
7.69803251e-04 4.23580589e-08 0.0e+00 0.0e+00 0.0e+00 0.0e+00
-7.67207830e-06 0.0e+00 0.0e+00 0.0e+00 0.0e+00 0.0e+00
0.0e+00 0.0e+00 0.0e+00 0.0e+00 0.0e+00 0.0e+00
0.0e+00 0.0e+00 0.0e+00 0.0e+00 0.0e+00 0.0e+00
0.0e+00 0.0e+00 0.0e+00 0.0e+00 0.0e+00 0.0e+00
#
# X astig
# SWAPPED
1.33063083e-03 1.68392660e-04 -8.55061473e-09 0.0e+00 0.0e+00 0.0e+00
-2.58073858e-05 -3.33276120e-06 0.0e+00 0.0e+00 0.0e+00 0.0e+00
-2.00120320e-08 0.0e+00 0.0e+00 0.0e+00 0.0e+00 0.0e+00
0.0e+00 0.0e+00 0.0e+00 0.0e+00 0.0e+00 0.0e+00
0.0e+00 0.0e+00 0.0e+00 0.0e+00 0.0e+00 0.0e+00
0.0e+00 0.0e+00 0.0e+00 0.0e+00 0.0e+00 0.0e+00
#
# Y astig
# SWAPPED
-8.35400173e-03 5.13194852e-04 -3.99141208e-06 0.0e+00 0.0e+00 0.0e+00
2.01150767e-04 -3.92886164e-08 0.0e+00 0.0e+00 0.0e+00 0.0e+00
-1.97495797e-06 0.0e+00 0.0e+00 0.0e+00 0.0e+00 0.0e+00
0.0e+00 0.0e+00 0.0e+00 0.0e+00 0.0e+00 0.0e+00
0.0e+00 0.0e+00 0.0e+00 0.0e+00 0.0e+00 0.0e+00
0.0e+00 0.0e+00 0.0e+00 0.0e+00 0.0e+00 0.0e+00
#
# X coma
# SWAPPED
2.31206647e-02 1.81284830e-04 -5.30494748e-06 0.0e+00 0.0e+00 0.0e+00
-1.39564501e-04 3.97479493e-06 0.0e+00 0.0e+00 0.0e+00 0.0e+00
-2.06559126e-06 0.0e+00 0.0e+00 0.0e+00 0.0e+00 0.0e+00
```

```
0.0e+00 0.0e+00 0.0e+00 0.0e+00 0.0e+00 0.0e+00
0.0e+00 0.0e+00 0.0e+00 0.0e+00 0.0e+00 0.0e+00
0.0e+00 0.0e+00 0.0e+00 0.0e+00 0.0e+00 0.0e+00
#
# Y coma
# SWAPPED
1.25930198e-02 -5.80506052e-04 5.25377957e-06 0.0e+00 0.0e+00 0.0e+00
-5.67486735e-04 4.09168135e-06 0.0e+00 0.0e+00 0.0e+00 0.0e+00
2.15934792e-06 0.0e+00 0.0e+00 0.0e+00 0.0e+00 0.0e+00
0.0e+00 0.0e+00 0.0e+00 0.0e+00 0.0e+00 0.0e+00
0.0e+00 0.0e+00 0.0e+00 0.0e+00 0.0e+00 0.0e+00
0.0e+00 0.0e+00 0.0e+00 0.0e+00 0.0e+00 0.0e+00
#
# WFC3 IR geometric distortion coefficients; used to convert
# detector X,Y position to telescope V2,V3
#
# V2,V3 (pupil) coordinates of reference position
#
  -1.0190  0.5070     = in arcsec
#
# Detector X,Y coordinates of reference position
#
   507 507  = pixels
#
# V2, V3 (pupil) coordinates of WFC3 IR camera center
#
  -1.0190  0.5070     = in arcsec
#
# X,Y -> V2 transform coefficients (4th order)
#
-7.834721E-6  1.354925E-1  -2.666651E-10  3.238674E-6  -1.381910E-10
3.737046E-14  1.843860E-11  4.087322E-13  3.758686E-12
0.0 0.0 0.0 0.0 0.0
#
# X,Y -> V3 transform coefficients
#
1.210825E-1   8.907462E-6   3.563704E-6   2.909743E-10  8.195221E-7
2.676912E-11 -3.854757E-13  1.336036E-11 -5.999974E-14
0.0 0.0 0.0 0.0 0.0
#
# V2,V3 -> X
#
4.775553E-4    7.380483E0  -7.414314E-8  -1.457858E-3  1.313760E-7
-1.377528E-10  5.729815E-7  -1.438840E-9  5.382542E-8
0.0 0.0 0.0 0.0 0.0
#
# V2,V3 -> Y
#
8.258834E0  -5.429441E-4  -2.009371E-3  1.718983E-7   -3.689799E-4
8.509658E-7  1.510508E-9   2.749957E-7  1.801569E-10
0.0 0.0 0.0 0.0 0.0
#
# Diffusion kernels to model the IPC effect
#
#  ********* Note - these are based on vac measurements kindly provided
#            by George Hartig in May 2008 - they are empirical and match what
was seen in thermal vac.
#            See WFC3 ISR 2008-41.
#
# These numbers are known to be a function of quadrant and readout, and not
determined as
# a function of wavelength. The values here are averages.
#
1.000  = Wavelength (microns) of kernel 1
#
# Kernel 1
#
```

```
0.0007 0.025  0.0007
0.025  0.897  0.025
0.0007 0.025  0.0007
#
1.300  = Wavelength (microns) of kernel 2
#
# Kernel 2
#
0.0007 0.025  0.0007
0.025  0.897  0.025
0.0007 0.025  0.0007
#
1.600  = Wavelength (microns) of kernel 3
#
# Kernel 3
#
0.0007 0.025  0.0007
0.025  0.897  0.025
0.0007 0.025  0.0007
#
# Additional field dependent charge diffusion relation coefficients
# Currently these are just place holders.
#
  2  = number of wavelengths at which coefficients are defined
#
#
  1.000  = wavelength 1
0.0 0.0 0.0 0.0 0.0 0.0
0.0 0.0 0.0 0.0 0.0 0.0
0.0 0.0 0.0 0.0 0.0 0.0
0.0 0.0 0.0 0.0 0.0 0.0
0.0 0.0 0.0 0.0 0.0 0.0
0.0 0.0 0.0 0.0 0.0 0.0
#
  1.600  = wavelength 2
0.0 0.0 0.0 0.0 0.0 0.0
0.0 0.0 0.0 0.0 0.0 0.0
0.0 0.0 0.0 0.0 0.0 0.0
0.0 0.0 0.0 0.0 0.0 0.0
0.0 0.0 0.0 0.0 0.0 0.0
0.0 0.0 0.0 0.0 0.0 0.0
```